

Vibrational spectra and structural features of carbene analogs $\text{El}^{\text{II}}(\text{OCH}_2\text{CH}_2\text{NMe}_2)_2$ and $\text{ClEl}^{\text{II}}\text{OCH}_2\text{CH}_2\text{NMe}_2$ ($\text{El}^{\text{II}} = \text{Ge}, \text{Sn}, \text{Pb}$)

R. R. Aysin,^a L. A. Leites,^{a*} S. S. Bukalov,^a V. N. Khrustalev,^a I. V. Borisova,^b
N. N. Zemlyanskii,^b A. Yu. Smirnov,^{b,c} and M. S. Nechaev^{b,c}

^aA. N. Nesmeyanov Institute of Organoelement Compounds, Russian Academy of Sciences,
28 ul. Vavilova, 119991 Moscow, Russian Federation.

Fax: +7 (499) 135 5085. E-mail: buklei@ineos.ac.ru

^bA. V. Topchiev Institute of Petrochemical Synthesis, Russian Academy of Sciences,
29 Leninsky prosp., 119991 Moscow, Russian Federation.

Fax: +7 (495) 633 8520

^cDepartment of Chemistry, M. V. Lomonosov Moscow State University,
Bldg. 3, 1 Leninskie Gory, 119991 Moscow, Russian Federation.

Fax: +7 (495) 932 8846. E-mail: nechaev@nmr.chem.msu.ru

Vibrational spectra of compounds of divalent Group 14 elements $\text{El}^{\text{II}}(\text{OCH}_2\text{CH}_2\text{NMe}_2)_2$ with $\text{El}^{\text{II}} = \text{Ge}$ (**1**), Sn (**2**), Pb (**3**) and $\text{ClEl}^{\text{II}}\text{OCH}_2\text{CH}_2\text{NMe}_2$ with $\text{El}^{\text{II}} = \text{Ge}$ (**4**) and Sn (**5**) were measured for the first time and analyzed within the framework of DFT calculations. Monomeric compounds **1** and **2** whose molecules are stabilized only through intramolecular coordination were confirmed to be isostructural. Unlike **1** and **2**, plumbylene **3** is a polymer in both solution and the crystalline state; the latter was confirmed by X-ray diffraction analysis. The $\nu_{\text{C-N}}$ stretching frequency in the CH_2NMe_2 fragment was shown to decrease by 80–100 cm^{-1} owing to the formation of the coordination bond $\text{El} \leftarrow \text{N}$. To elucidate the mechanism of a dynamic *flip-flop* process suggested earlier based on the broadening of some signals in the NMR spectra of compounds **1** and **4**, the Raman spectra of solutions of compounds **1** and **2** in THF and Py were obtained. These experiments revealed no equilibrium with participation of a stable form with one coordination bond $\text{El} \leftarrow \text{N}$ cleaved along with the starting molecule. This is consistent with the results of the corresponding quantum chemical calculations of thermodynamic parameters. A somewhat different, more probable mechanism of the dynamic process was proposed, which involves an overturn of the CH_2NMe_2 fragment with cleavage of the $\text{El} \leftarrow \text{N}$ bond in the transition state only.

Key words: germynes, stannynes, plumbylenes, vibrational spectra, X-ray diffraction analysis, density functional theory, quantum chemical calculations, dynamic *flip-flop* process.

Heavier carbene analogs (CA) including germynes, stannynes, and plumbylenes are an important class of nonclassical organoelement compounds. Earlier,¹ a new-type germylene and stannylene $\text{El}(\text{OCH}_2\text{CH}_2\text{NMe}_2)_2$ with $\text{El} = \text{Ge}$ (**1**) and Sn (**2**) have been synthesized and characterized. The molecules **1** and **2** are stabilized only through intramolecular coordination, the carbenoid atom being sterically unshielded. According to the X-ray diffraction data (Fig. 1),¹ compounds **1** and **2** in the crystal are isostructural and exist as monomers. The El atom is four-coordinate due to two covalent $\text{El}-\text{O}$ bonds and two intramolecular coordination $\text{N} \rightarrow \text{El}$ bonds of equal length (unlike the corresponding Sn^{II} compounds with bulky substituents^{2,3}).

More recently, chlorides $\text{ClEl}^{\text{II}}\text{OCH}_2\text{CH}_2\text{NMe}_2$ with $\text{El} = \text{Ge}$ (**4**) and Sn (**5**) have been synthesized. It was

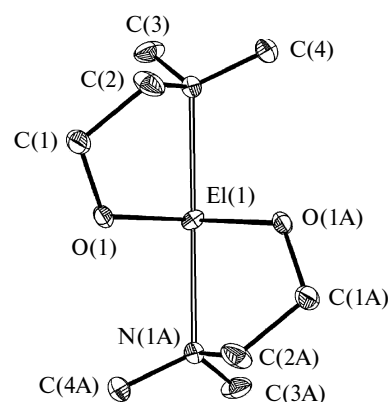


Fig. 1. Structures of carbene analogs $\text{El}(\text{OCH}_2\text{CH}_2\text{NMe}_2)_2$ with $\text{El} = \text{Ge}$ (**1**) and Sn (**2**) determined by X-ray diffraction analysis.¹

found that germylene **4** is monomeric,⁴ the formation of an intramolecular coordination bond $\text{El} \leftarrow \text{N}$ being sufficient to stabilize its molecule. However, the corresponding tin derivative **5** is a centrosymmetric dimer formed also due to intermolecular coordination bonds $\text{El} \leftarrow \text{O}$.⁵ Compounds related to **1** and **2** were also reported.^{6–8} The ^1H and ^{13}C NMR spectra of compounds **1** and **4** in solution exhibit a number of broadened signals.^{1,4,6,8c} By analogy with the published data,⁹ it was suggested^{1,4,6,8} that a fast process of cleavage and formation of the coordination bond $\text{El} \leftarrow \text{N}$ (the so-called "flip-flop" process) occurs in solutions of compounds **1**, **2**, and **4**. According to quantum chemical calculations,¹ the molecule with one "free" $-\text{CH}_2-\text{CH}_2-\text{NMe}_2$ group corresponds to a local minimum on the potential curve. In this connection, it was of interest to reveal the flip-flop process by means of vibrational spectra because the characteristic time of IR and Raman spectroscopies is a few orders of magnitude shorter than that of NMR spectroscopy.

The aims of the present work were to synthesize and structurally characterize plumbylene $\text{Pb}(\text{OCH}_2\text{CH}_2\text{NMe}_2)_2$ (**3**), an analog of compounds **1** and **2**, and to perform a thorough comparative study of the previously unknown vibrational spectra of compounds **1–5** measured not only in the crystalline phase, but also in solutions in order to investigate structural features of the systems in question and to detect the flip-flop process if possible.

Experimental

All operations were performed *in vacuo* or in the atmosphere of dry argon free from oxygen traces using conventional Schlenk technique. Pyridine and THF were distilled over sodium prior to use.

The synthesis of compounds **1**, **2**, **4**, and **5** was reported earlier.^{1,4,5} Compound **3** was obtained by alcoholysis of lead amide $\text{Pb}[\text{N}(\text{SiMe}_3)_2]_2$ (see Ref. 10) with (dimethylamino)-ethanol in hexane.

NMR spectra were recorded using a Bruker Am460 spectrometer for solutions in C_6D_6 . Vibrational spectra of the samples unstable in air were recorded immediately after their recrystallization from hexane.

The Raman spectra of crystalline compounds and solutions were measured using the samples sealed in capillaries filled with dry argon. The spectra in the region $50\text{--}3500\text{ cm}^{-1}$ were recorded on a last-generation Horiba Jobin–Yvon LabRAM 300 laser Raman spectrometer equipped with a microscope, a video camera, and a cooled CCD detector. The 632.8 nm line of a He–Ne laser (power at most 5 mW) was used for excitation of the spectra.

IR spectra in the region $300\text{--}3600\text{ cm}^{-1}$ were registered using a Carl Zeiss Specord M-82 spectrophotometer; frequency corrections were made with the use of the reference polystyrene spectrum. The IR spectra of solid samples were obtained for thin films sublimed on a cooled CsI substrate in a vacuum cryostat.

Geometry optimization, the normal coordinate analysis (NCA) in a harmonic approximation, and calculations of the IR and Raman intensities were carried out using the GAUSSIAN 03

C.01 program¹¹ within the framework of the density functional theory (DFT) with the PBE and PBE0 functionals.¹² The 6-311G(d,p) basis set was used for the H, C, N, O, and Cl atoms¹³ and for one metal atom, Ge. For other metal atoms, Sn and Pb, the cc-pVTZ-pp basis set¹⁴ was employed. The calculated and experimental vibrational frequencies are in reasonable agreement although no scaling factors were applied. Moreover, calculations reproduce the Raman and IR intensities quite correctly. Calculations of the potential energy distribution (PED) over internal vibrational coordinates were carried out with the NCA99 program.¹⁵

Bis[*N*-(dimethylamino)ethoxy]plumbylene (3**).** To a solution of bis[bis(trimethylsilyl)amino]plumbylene (2.79 g , 5.3 mmol) in hexane (35 mL), an excess of dimethylaminoethanol (1.5 mL , 1.33 g , 14.9 mmol) was added dropwise with stirring in a water bath ($20\text{ }^\circ\text{C}$). After 12 h at $20\text{ }^\circ\text{C}$, the white powder was filtered off, dried *in vacuo*, and recrystallized from hexane at $-12\text{ }^\circ\text{C}$. The yield was 1.5 g (74%), white crystals soluble in conventional organic solvents and stable under anaerobic conditions. M.p. $67\text{--}68\text{ }^\circ\text{C}$. ^1H NMR (C_6D_6), δ (J/Hz): 2.18 (s, 12 H , Me_2N , $^1J_{\text{CH}} = 132.7$); 2.52 (t, 4 H , CH_2N , $^3J_{\text{H,H}} = 5.1$); 4.53 (t, 4 H , CH_2O , $^3J_{\text{H,H}} = 5.1$). ^{13}C NMR (C_6D_6), δ : 45.23 (Me_2N), 61.65 (CH_2N), 65.72 (CH_2O). ^{207}Pb NMR (C_6D_6), δ : -309.9 . Since compound **3** is extremely sensitive to oxygen and moist air, attempts to perform elemental analysis have failed.

X-ray diffraction study of complex **3.** Crystals of compound **3** ($\text{C}_8\text{H}_{20}\text{N}_2\text{O}_2\text{Pb}$, $M = 383.45$) are triclinic ($0.30 \times 0.03 \times 0.03\text{ mm}^3$), space group $P\bar{1}$, at $T = 100\text{ K}$: $a = 6.2328(19)\text{ \AA}$, $b = 9.362(3)\text{ \AA}$, $c = 11.007(3)\text{ \AA}$, $\alpha = 97.979(6)^\circ$, $\beta = 104.615(6)^\circ$, $\gamma = 92.552(6)^\circ$, $V = 613.4(3)\text{ \AA}^3$, $Z = 2$, $d_{\text{calc}} = 2.076\text{ g cm}^{-3}$, $F(000) = 360$, $\mu = 13.729\text{ mm}^{-1}$. The unit cell parameters and the intensities of 6517 reflections were measured on a Bruker APEX II CCD automated diffractometer ($\lambda(\text{Mo-K}\alpha)$ -radiation, graphite monochromator, φ - and ω -scans, $2\theta_{\text{max}} = 56^\circ$). The absorption correction was applied analytically (crystal evaluation by indexing its faces).¹⁶ The structure was solved by the direct method and refined by the full-matrix least squares method with respect to F^2 in the anisotropic approximation for non-hydrogen atoms. Hydrogen atoms were located geometrically and refined in the riding model with fixed thermal parameters ($U_{\text{iso}}(\text{H}) = 1.5U_{\text{eq}}(\text{C})$ for CH_3 groups and $U_{\text{iso}}(\text{H}) = 1.2U_{\text{eq}}(\text{C})$ for CH_2 groups). The final R -factor values are as follows: $R_1 = 0.061$ for 2585 independent reflections with $I > 2\sigma(I)$ and $wR_2 = 0.154$ for all 2867 independent reflections; $\text{GOF} = 1.010$. All calculations were carried out using the SHELXTL program package.¹⁷ Tabulated atomic coordinates, bond lengths, bond angles, and anisotropic thermal parameters for compound **3** were deposited at the Cambridge Structural Database.

Results and Discussion

The complete IR and Raman spectra of compounds **1–3** (for both crystalline samples and solutions in THF and Py) as well as the Raman spectra of compounds **4** and **5** reported in the present work were obtained for the first time. For correct normal mode assignment and structure determination, DFT quantum chemical calculations of the molecular geometries, normal mode frequencies and eigenvectors (NCA), their Raman and IR intensities, as

well as the PED were carried out in a harmonic approximation. The calculated and experimental frequencies are in reasonable agreement, although no scale factors were introduced (theoretical frequencies are underestimated by about $10\text{--}20\text{ cm}^{-1}$). The structure of compound **3** was established by X-ray diffraction analysis.

Germynes 1 and 4 and stannylenes 2 and 5. In the spectral region above 600 cm^{-1} where the bands corresponding to the vibrations of the $\text{CH}_2\text{CH}_2\text{NMe}_2$ fragment are situated, the spectra of **1** and **2** are very similar (Figs 2–4). Noteworthy are four intense IR bands at nearly 780 , 885 , 950 , and 1037 cm^{-1} ; three of them are of medium intensity in the Raman spectrum. According to the NCA data, the strong Raman line at about 780 cm^{-1} and the strong IR band at 775 cm^{-1} correspond to a symmetric vibration of complex origin with a large contribution (more than 50% in PED) from the stretching coordinates of the three C–N bonds in the fragment $-\text{CH}_2\text{NMe}_2$ (this vibration is conditionally denoted as $\nu^s_{\text{C-N}}$). The Raman line corresponds to the in-phase vibration in two fragments $-\text{CH}_2\text{NMe}_2$ while the IR band corresponds to their out-of-phase combination. The band at $\sim 950\text{ cm}^{-1}$ corresponds to an analogous antisymmetric vibration of mixed

origin with a contribution from $\nu^{\text{as}}_{\text{C-N}}$ of about 30% (denoted as $\nu^{\text{as}}_{\text{C-N}}$, Table 1). The normal mode at nearly 885 cm^{-1} has a complex eigenvector and includes large contributions from the C–C and C–O stretching coordinates as well as from angle deformations in the CH_2 groups (this mode is denoted as ρ_{CH_2}). Strong IR bands at 1037 and nearly 1085 cm^{-1} correspond to mixed modes with a significant participation of the C–O bonds. The bands in the region $\nu > 1100\text{ cm}^{-1}$ correspond to the coupled $\nu_{\text{C-C}}$ stretching and δ_{CH_2} deformation vibrations.

The spectral region $\nu < 600\text{ cm}^{-1}$ deserves particular attention because it was suggested to contain the $\nu(\text{El-O})$ stretching vibrations. However, according to our calculations, these vibrations are strongly coupled; the El–O stretching coordinate appears to participate in four normal modes, its contribution to their potential energies is more than 10%. By analogy with the notations used in the analysis of the five-membered ring vibrations,¹⁸ the strongest Raman line at 522 cm^{-1} of compound **1** should be assigned to the in-phase "breathing" mode of two five-membered rings GeOCCN . The ν^s_{GeO} contribution to the PED of this normal vibration is 50%. The band at about 485 cm^{-1} in the spectrum of compound **1** corresponds to

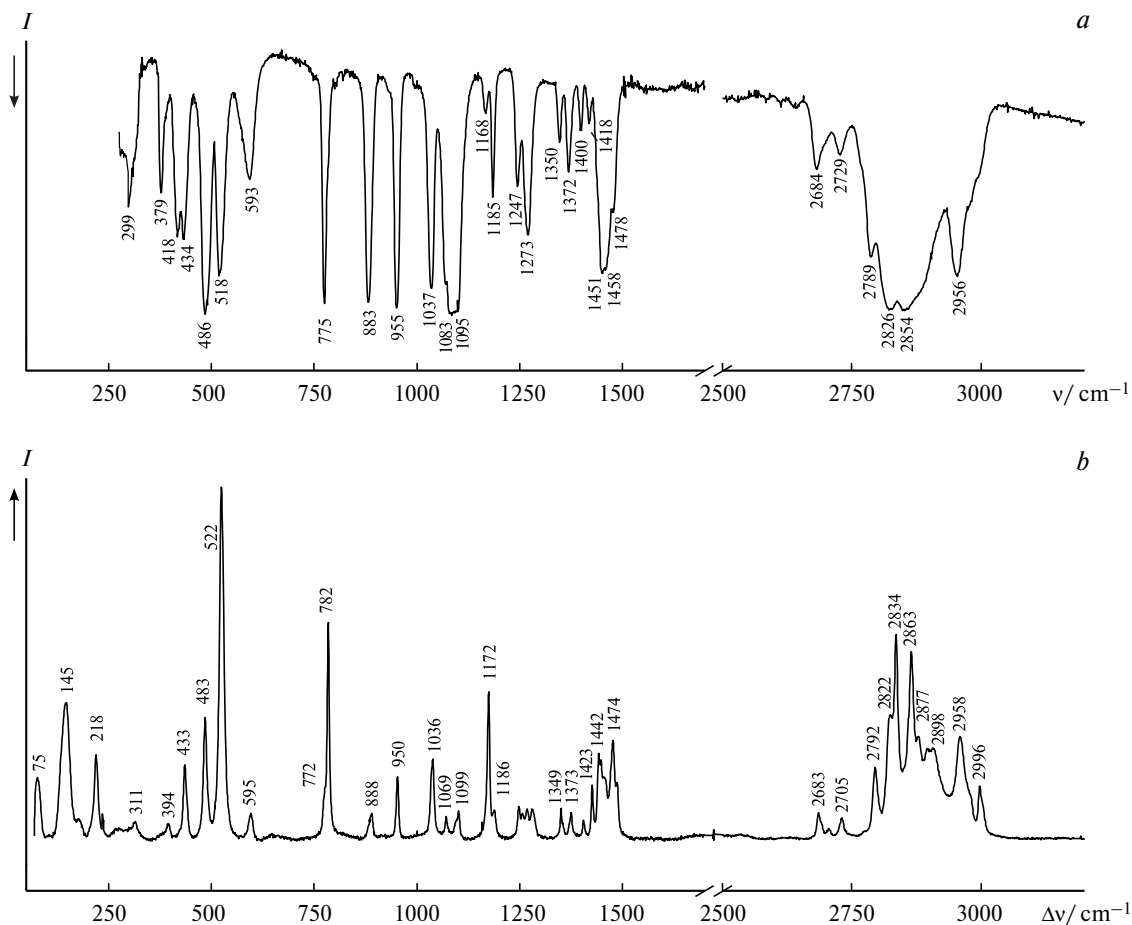


Fig. 2. IR spectrum (a) and the Raman spectrum (b) of crystalline $\text{Ge}(\text{OCH}_2\text{CH}_2\text{NMe}_2)_2$ (**1**).

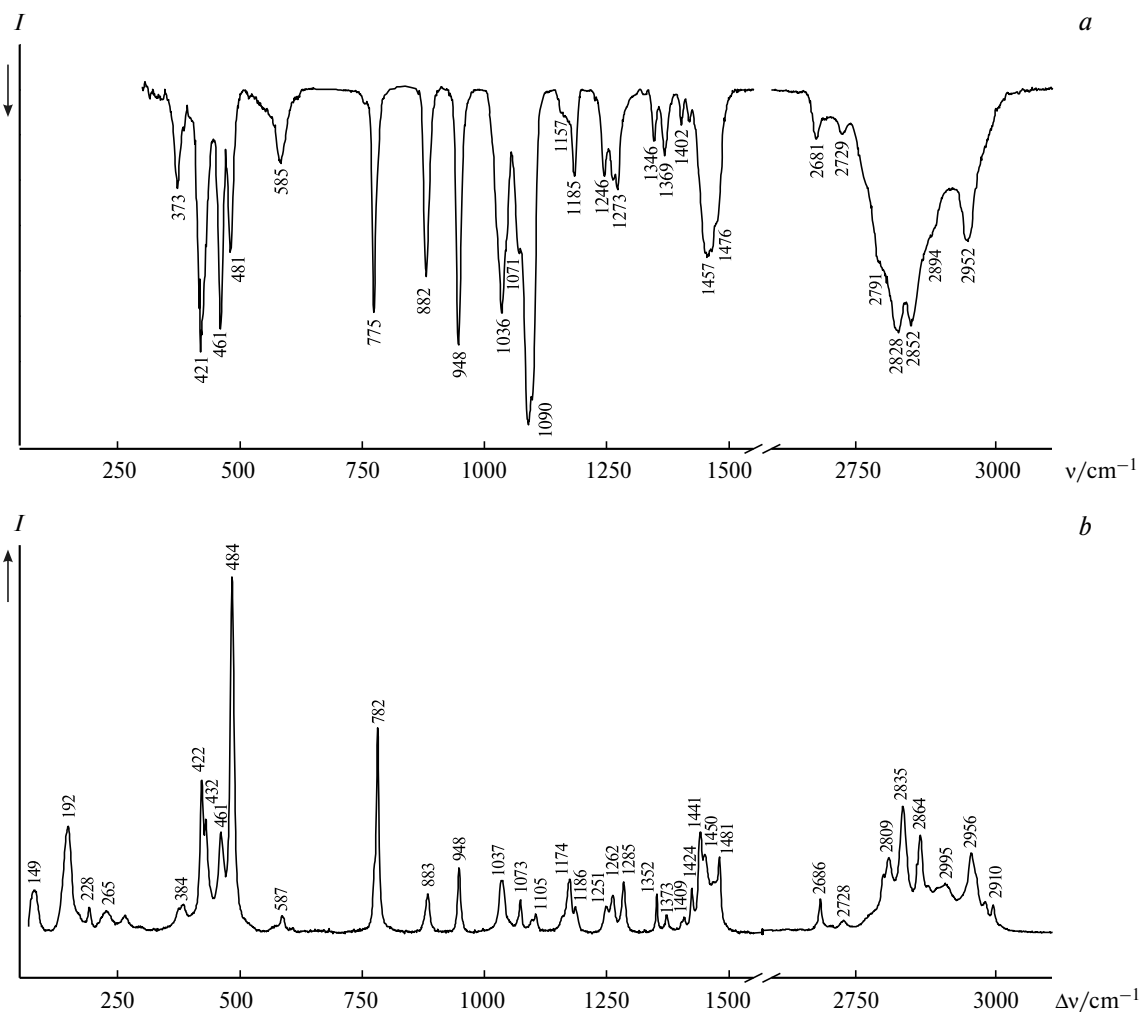
Table 1. Assignment of analytically important bands in the IR/Raman spectrum of germylene **1**

Frequency/cm ⁻¹			Assignment	PED
IR	Raman	Calculated		
486 s	483 m	451	Out-of-phase "breathing" vibration of two chelate rings	36% $\nu^{\text{as}}_{\text{GeO}}$ + 26% δ_{GeOC} + 10% δ_{CNC}
518 s	522 s	482	In-phase "breathing" vibration of two chelate rings	50% $\nu^{\text{s}}_{\text{GeO}}$ + 20% δ_{GeOC}
593 m	595 w	575	Ring deformation	30% δ_{OCC} + 22% δ_{GeOC} + 12% ρ_{CH_2}
775 s	772 w	761	Out-of-phase $\nu^{\text{s}}_{\text{CN}}$ stretching vibration of two CH_2NMe_2 groups	56% $\nu^{\text{s}}_{\text{CN}}$ + 16% ρ_{CH_2}
—	782 s	771	In-phase $\nu^{\text{s}}_{\text{CN}}$ stretching vibration of two CH_2NMe_2 groups	54% $\nu^{\text{s}}_{\text{CN}}$ + 16% ρ_{CH_2}
883 s	888 w	867	Coupled vibration with large contributions from the ρ_{CH_2} and ν_{CC} stretching coordinates	38% ρ_{CH_2} + 24% ν_{CC} + 12% ν_{CO}
955 s	950 m	937	Coupled vibration with large contributions from the ρ_{CH_2} and $\nu^{\text{as}}_{\text{CN}}$ coordinates	37% ρ_{CH_2} + 28% $\nu^{\text{as}}_{\text{CN}}$ + 14% ν_{CC}

Note. Band intensities: s is strong, m is medium, and w is weak.

an out-of-phase "breathing" mode of the two rings ($\nu^{\text{as}}_{\text{GeO}}$ contribution to the PED is 36%). In the Raman spectrum of compound **2**, the corresponding vibrations with large

ν_{SnO} contributions are the bands at 484 and 461 cm⁻¹, respectively. It is noteworthy that in both spectra the frequency of the symmetric $\nu^{\text{s}}_{\text{EIO}}$ vibration is higher than that

**Fig. 3.** IR spectrum (a) and the Raman spectrum (b) of crystalline $\text{Sn}(\text{OCH}_2\text{CH}_2\text{NMe}_2)_2$ (**2**).

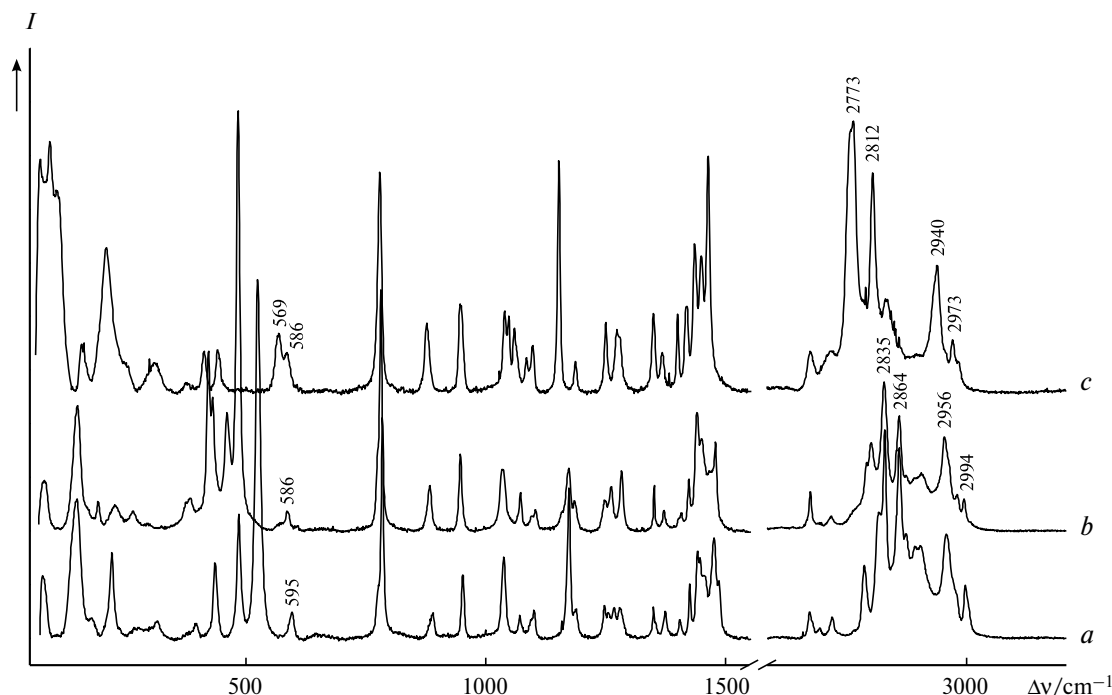


Fig. 4. The Raman spectra of crystalline samples of compounds **1** (a), **2** (b), and **3** (c).

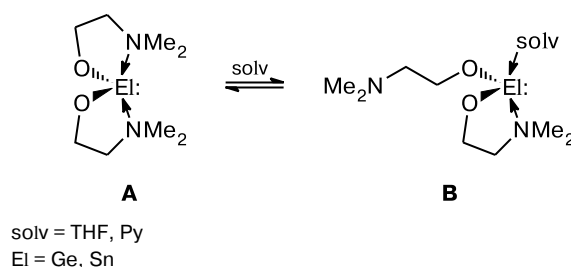
of $\nu_{\text{ElO}}^{\text{as}}$. This means that the inversion of the frequencies of the $\nu(\text{El}-\text{X})$ stretching vibrations characteristic of the spectra of carbene analogs¹⁹ holds also for the stretching vibrations of the GeO_2 and SnO_2 fragments in the complexes **1** and **2** (despite the mixed character of these modes). A coupled vibration at about 590 cm^{-1} for compounds **1** and **2** includes nearly equal contributions from the deformations of the $\text{El}-\text{O}-\text{C}$ and $\text{O}-\text{C}-\text{C}$ angles. The assignment of the key bands in the spectrum of **1** is given in Table 1. The mode eigenvectors in the spectrum of **2** are basically the same, but particular contributions to the PED are somewhat different.

The spectrum of chlorogermylene **4** in the region $600\text{--}1500\text{ cm}^{-1}$ (Fig. 5, a) is similar to the spectrum of **1**, but the "breathing" frequency of the only ring in **4** is increased to 556 cm^{-1} due to the effect of the Cl atom. The $\text{Ge}-\text{Cl}$ stretching vibration is not pure; the corresponding coordinate participates mainly in the normal modes at 325 and 288 cm^{-1} .

The spectrum of dimeric chlorostannylene **5** differs from the spectrum of **2** in the low-frequency region where coupled vibrations with participation of the $\text{Sn}-\text{Cl}$ and $\text{Sn}-\text{O}$ bonds are situated (see Fig. 5, b).

On the so-called flip-flop process. Based on the results of calculations¹ and on the published concepts,^{1,8d} we first modeled a possible *flip-flop* process as cleavage of one coordination bond $\text{El} \leftarrow \text{N}$ in the initial structure **A** and formation of a complex with the solvent molecule (**B**) provided the existence of the corresponding equilibrium $\text{A} \rightleftharpoons \text{B}$ (Scheme 1).

Scheme 1



The thermodynamic parameters of this process involving compounds **1** and **2** were computed and NCA calculations for the vibrations of the molecules **1** and **2** with one ring open were also performed. According to the NCA results, if the "terminal" nitrogen atom is not coordinated to the El atom, the frequency of the symmetric vibration $\nu_{\text{C-N}}^{\text{s}}$ should increase to nearly 850 cm^{-1} . This result is confirmed experimentally, viz., by the Raman spectrum of a model compound $\text{Me}_2\text{NCH}_2\text{CH}_2\text{NMe}_2$ (TMEDA) (Fig. 6) with its obviously "free" nitrogen atoms. In this spectrum, the frequency of the polarized line corresponding to the $\nu_{\text{C-N}}^{\text{s}}$ vibration is 875 cm^{-1} .

Given the equilibrium $\text{A} \rightleftharpoons \text{B}$, some spectral lines should be doubled owing to the presence of vibrations of both coordinated and "free" $\text{CH}_2\text{CH}_2\text{NMe}_2$ fragments.

Now we will analyze the energy parameters of the *flip-flop* process in solution, as modeled by Scheme 1. According to the calculations for isolated molecules **1** and **2**,¹ the total energy difference between the forms **A** and **B** (one

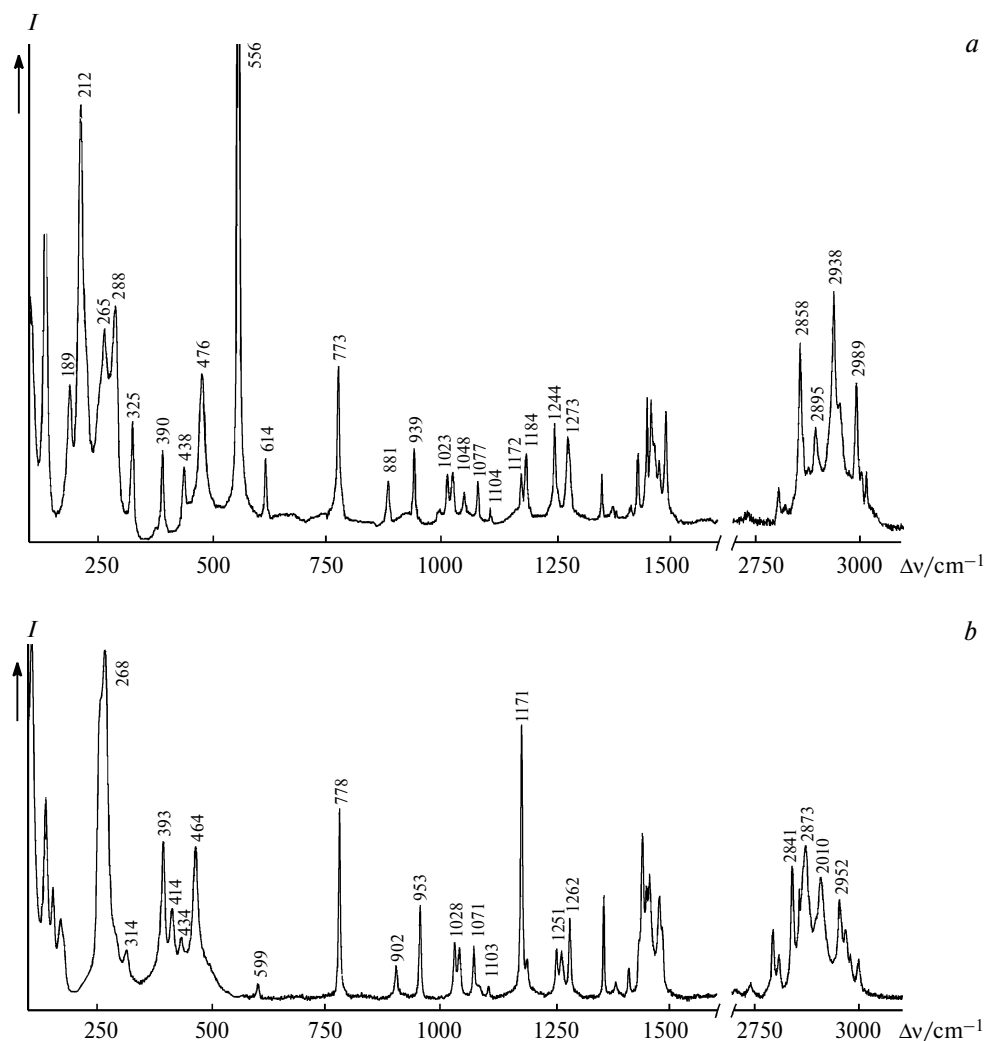


Fig. 5. The Raman spectra of crystalline (a) $\text{ClGeOCH}_2\text{CH}_2\text{NMe}_2$ (**4**) and (b) $\text{ClSnOCH}_2\text{CH}_2\text{NMe}_2$ (**5**).

ring being "open", no coordination with the solvent) is 7.6 and 10.2 kcal mol⁻¹, respectively. The DFT calculations of the enthalpy and the Gibbs free energy of the process $\mathbf{A} \rightleftharpoons \mathbf{B}'$ in the gas phase gave the values presented in Table 2. The process appears to be thermodynamically unfavorable (ΔH , $\Delta G > 0$). It is evident that the "open" form will not be

observed in solutions in inert solvents. One could expect that in solutions in polar aprotic solvents, the ΔH and ΔG values will decrease to such an extent that the equilibrium in question would become feasible.

However, from the data of Table 2 it follows that the process $\mathbf{A} \rightleftharpoons \mathbf{B}$ (solv = THF and Py) is also characterized

Table 2. Calculated ΔE_{tot} values and thermodynamic parameters ΔH and ΔG (kcal mol⁻¹) of the process $\mathbf{A} \rightleftharpoons \mathbf{B}$ (see Scheme 1) for compounds **1** and **2** at room temperature

Compound	Functional	In the gas phase without solvent (B')			Solv = THF			Solv = Py		
		ΔE_{tot}	ΔH	ΔG	ΔE_{tot}	ΔH	ΔG	ΔE_{tot}	ΔH	ΔG
$\text{Ge}(\text{OCH}_2\text{CH}_2\text{NMe}_2)_2$ (1)	PBE	8.63	9.07	6.42	2.74	3.68	12.59	0.49	1.47	9.74
	PBE0	8.96	9.40	6.43	3.76	4.10	13.67	1.02	2.01	10.25
$\text{Sn}(\text{OCH}_2\text{CH}_2\text{NMe}_2)_2$ (2)	PBE	11.58	12.10	9.00	3.45	4.53	11.43	0.74	1.77	9.92
	PBE0	12.25	12.77	9.59	4.33	5.41	12.35	1.30	2.33	10.51

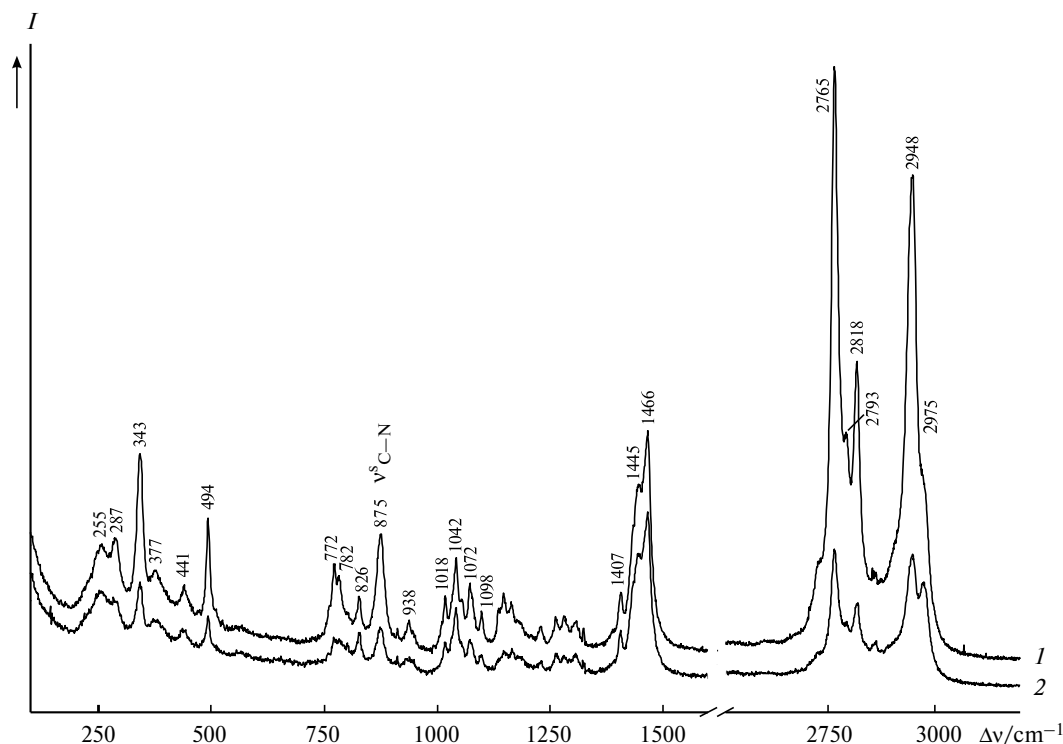


Fig. 6. The Raman spectrum of TMEDA: a parallel (1) and a perpendicular polarization (2).

by positive ΔG values. This conclusion is consistent with the experimental Raman results for the solutions of compounds **1** and **2** in these solvents, where no changes were observed in the region 700–1000 cm⁻¹ (see, e.g., Fig. 7) compared to the spectra of the crystalline samples.

Thus, no indications of presence of the form **B** with the "open" coordination bond $\text{El} \leftarrow \text{N}$, *i.e.*, of the suggested equilibrium $\text{A} \rightleftharpoons \text{B}$, were observed in the Raman spectrum under the conditions studied. It should be noted that the proposed cleavage of the coordination bond $\text{N} \rightarrow \text{Ge}$ with an energy of 16 kcal mol⁻¹ (see Ref. 4) in the solution of compound **4** in CD₂Cl₂ also seems to be thermodynamically impossible. Clearly, the actual mechanism of the dynamic process in molecules **1**, **2**, and **4** (the so-called "flip-flop equilibrium"^{1,8d}) differs from that proposed in Scheme 1. In this connection, the published data²⁰ are of interest where the mechanism of the dynamic process for a compound related to **4**, namely, diphosphagermylene with a three-coordinate Ge atom and a chelate six-membered ring $\{\text{R}(\text{C}_6\text{H}_4\text{-2-CH}_2\text{NMe}_2)\text{P}\}\text{GeCl}$ are considered.

One can suggest yet another mechanism of the dynamic flip-flop process in the molecules in question. It also leads to averaging of signals of the two methyl groups at the nitrogen atom and broadening of signals of the CH₂ groups in the NMR spectra. If the structures of molecules **1**, **2**, and **4** were rigid, the two methyl groups at one nitrogen atom would be nonequivalent because one of them is closer to the stereochemically active lone electron pair

(LP) of the El atom than the other. However, the NMe₂ group appears in the ¹H and ¹³C NMR spectra as a singlet which widens with temperature,^{1,4} thus clearly pointing to the methyl group exchange. This process can be represented as an overturn of the CH₂NMe₂ fragment with a significant elongation of the El...N distance, *i.e.*, cleavage of the $\text{El} \leftarrow \text{N}$ coordination bond in the transition state only (Fig. 8).

The calculated activation energy of this process (ΔE_{tot}) is low (see below), which makes it quite probable. The broadening of the signals of CH₂ groups can be explained by the concomitant conformational transition about the C—C bond in the nonplanar chelate five-membered ring EIOCCN.²¹

Molecule	ΔE_{tot} /kcal mol ⁻¹
Ge(OCH ₂ CH ₂ NMe ₂) ₂ (1)	9.3
Sn(OCH ₂ CH ₂ NMe ₂) ₂ (2)	14.7
ClGeOCH ₂ CH ₂ NMe ₂ (4)	24.2

Plumbylene (3). Vibrational spectra and structure. As shown above, the spectra of **1** and **2** in the regions 550–1500 and 2700–3100 cm⁻¹ are very similar to each other; this is consistent with the fact that these compounds are isostructural. According to the NCA results for an isostructural monomeric plumbylene **3m**, the spectral pattern in the regions mentioned above should not alter on going from **1** and **2** to **3m**. However, the Raman spectrum of a crystalline sample of compound **3** is significantly different from those of **1** and **2** and exhibits a low-frequency shift of

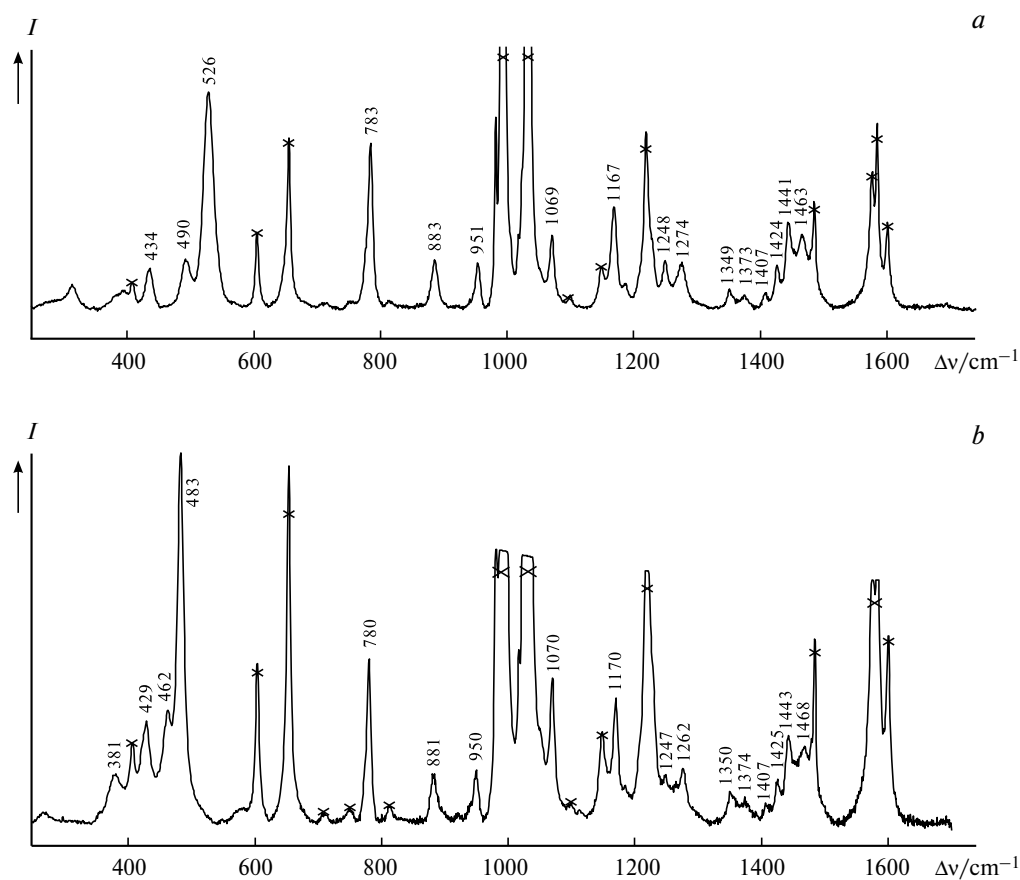


Fig. 7. The Raman spectra of solutions of compounds **1** (a) and **2** (b) in Py; the pyridine lines are denoted by "×".

the most intense bands corresponding to the $\nu_{\text{C-H}}$ vibrations (from about 60 to nearly 15 cm^{-1}) compared to the spectra of compounds **1** and **2** (see Fig. 4). The Raman spectrum of plumblyene **3** is also more complicated in the region $1000\text{--}1200\text{ cm}^{-1}$ where coupled vibrations with

contributions from the coordinates $\nu_{\text{C-O}}$, $\nu_{\text{C-N}}$, and δ_{CH} are situated, and exhibits duplication of the line near 590 cm^{-1} corresponding to the El-O-C and O-C-C angle deformations. Interestingly, no strong lines were observed in the region $400\text{--}550\text{ cm}^{-1}$. Based on these data, we have assumed that plumblyene **3** is not isostructural to compounds **1** and **2**. Indeed, X-ray diffraction data have shown that plumblyene **3** is not a monomer, but a coordination polymer formed by intermolecular coordination bonds $\text{Pb} \leftarrow \text{O}$ (see below).

To elucidate the spectral changes due to plumblyene polymerization, NCA calculations were carried out for the tetramer **3p** whose central fragment can model to some extent the polymer **3**.

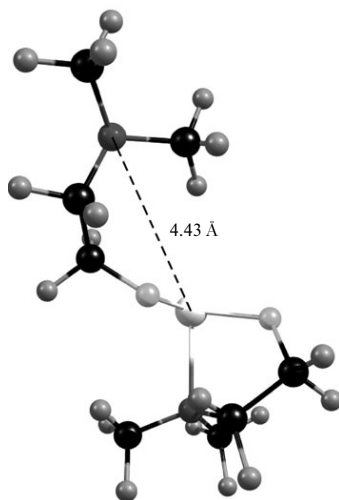
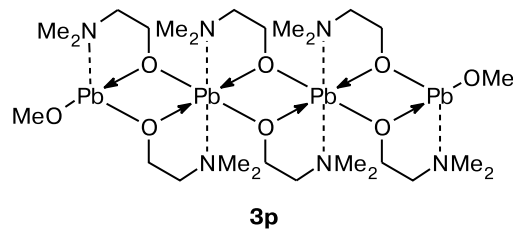


Fig. 8. Transition-state geometry for the *flip-flop* process resulting in "exchange" of methyl groups in compound **1**.



The NCA calculations showed that the ν_{CH} stretching frequencies of **3p** are lower than those of monomer **3m**.

Thus, the low-frequency shift of ν_{CH} observed in the experimental spectrum **3** is consistent with the polymeric structure of plumbylene **3**.

As mentioned above, the strong Raman lines at 522 cm^{-1} in the spectrum of **1** and at 484 cm^{-1} in the spectrum of **2** correspond to the mixed modes localized in the chelate five-membered rings $\text{El}^{\text{II}}\text{OCCN}$ and having the major contribution from the stretching coordinates $\nu_{\text{El-O}}^s$. The NCA results for a virtual monomer **3m** predict the frequency of 442 cm^{-1} for the similar mixed mode with the major contribution of the $\nu_{\text{Pb-O}}^s$ coordinate. The absence of such a Raman line in the spectrum of polymer **3** can be explained by strong intermolecular coordination $\text{O}\rightarrow\text{Pb}$, which should unavoidably alter the eigenvectors of normal modes and their frequencies.

The Raman spectrum of a saturated solution of plumbylene **3** in Py (Fig. 9) does not differ significantly from the spectrum of a crystalline sample. Therefore, no depolymerization of **3** occurs in this solution. This is not surprising because the DFT PBE0 calculated energy of dissociation of the tetramer **3p** to two equal fragments is $17.1\text{ kcal mol}^{-1}$.

Crystal structure of $\text{Pb}(\text{OCH}_2\text{CH}_2\text{NMe}_2)_2$ (3**).** According to X-ray diffraction data, the complex $\text{Pb}(\text{OCH}_2\text{CH}_2\text{NMe}_2)_2$ is an infinite one-dimensional polymer formed by intermolecular coordination bonds

$\text{Pb}\leftarrow\text{O}$ (Fig. 10). All the alkoxy ligands are bridging ones, no terminal alkoxy substituents are present. The monomeric fragments $\text{Pb}(\text{OCH}_2\text{CH}_2\text{NMe}_2)_2$ in the coordination polymer are connected by centers of inversion located at the centers of the four-membered rings $\text{Pb}-(\mu\text{-O})_2\text{-Pb}$, and, hence, they are crystallographically equivalent. The lead atom, Pb^{II} , has a distorted trigonal-bipyramidal configuration with a stereochemically active LP in the equatorial position. Selected geometric parameters of polymer **3** are listed in Table 3. The values of the bond angles $\text{O}_{\text{ax}}\text{-Pb-O}_{\text{ax}}$ ($150.3(2)^\circ$) and $\text{O}_{\text{eq}}\text{-Pb-O}_{\text{eq}}$ ($89.3(3)^\circ$) are smaller than those in an ideal trigonal bipyramid (180 and 120° , respectively). This confirms the presence of equatorial LP.

The axial distances Pb-O ($2.390(7)$ and $2.478(8)\text{ \AA}$) are longer than the equatorial ones ($2.224(7)$ and $2.249(8)\text{ \AA}$). Following Haaland's classification,²² the lead-oxygen bonds in structure **3** can be interpreted as dative $\text{Pb}\leftarrow\text{O}$ (long) bonds and covalent Pb-O (short) ones. Since every alkoxy ligand is involved in the formation of one axial and one equatorial bond, the bridging oxygen atoms are arranged asymmetrically relative to the lead atoms. Structurally, polymer **3** is very similar to the previously studied related polymer $[\text{Pb}(\text{OCH}_2\text{CH}_2\text{OMe})_2]_\infty$ (**6**) (see Table 3).²³

The values of the interatomic distances $\text{Pb}\dots\text{N}$ suggest that potentially bidentate dimethylaminoethoxy ligands

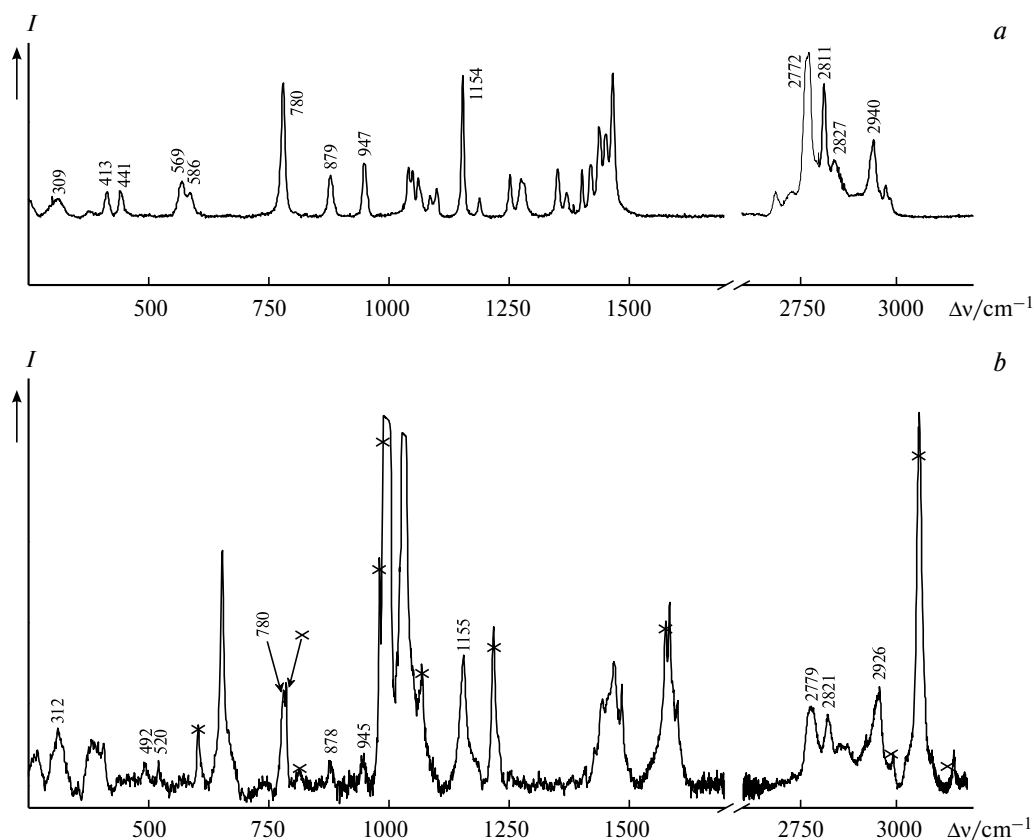


Fig. 9. The Raman spectrum of crystalline plumbylene **3** (a) and its solution in Py (b); the pyridine lines are denoted by "x".

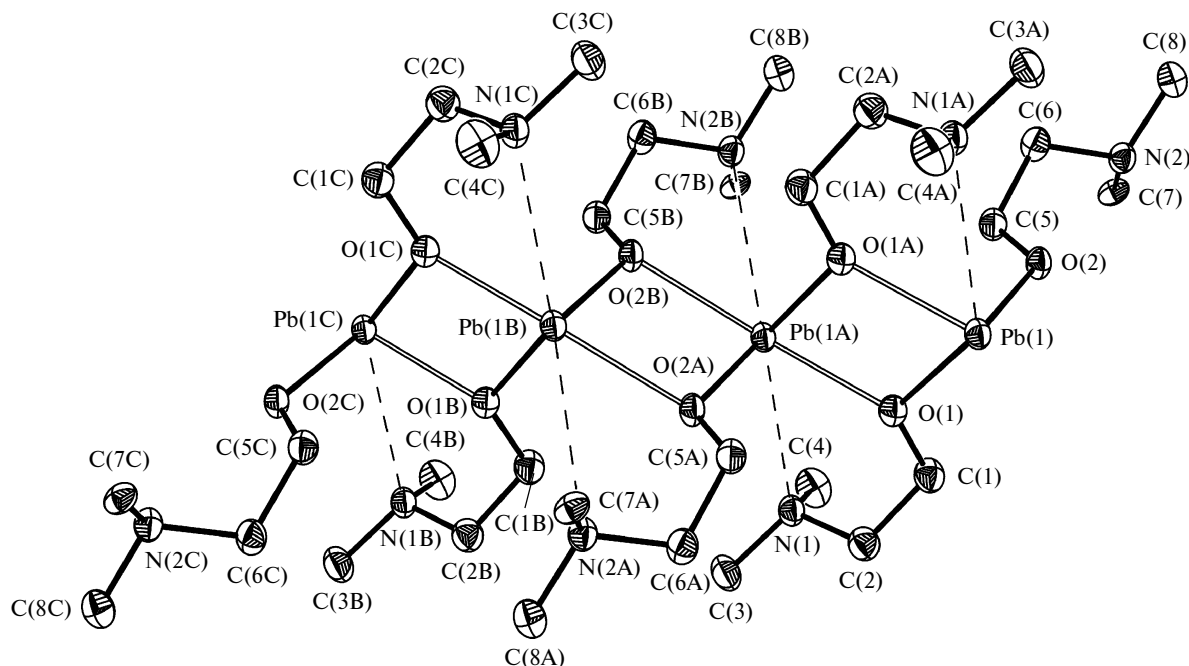


Fig. 10. The structure of coordination polymer **3** according to X-ray diffraction data.

in structure **3** form no chelate rings involving the donor nitrogen atoms. However, noteworthy is an interesting structural feature of **3**, namely, the LPs of nitrogen atoms are directed toward lead atoms of neighboring fragments $\text{Pb}(\text{OCH}_2\text{CH}_2\text{NMe}_2)_2$.

Table 3. A comparison of geometric parameters in the structure of compounds $[\text{Pb}(\text{OCH}_2\text{CH}_2\text{X})_2]_\infty$ ($\text{X} = \text{OMe}$ (**6**), NMe_2 (**3**))

Parameter	X = OMe (see Ref. 22)	X = NMe ₂
Bond length	<i>d</i> /Å	
Pb—O	2.234(4)	2.224(7), 2.249(8)
Pb←O	2.440(5)	2.390(7), 2.478(7)
Pb...X	3.170(5)	3.060(7), 3.240(7)
Pb...Pb	3.824(1)	3.824(1), 3.822(1)
Angle	ϕ /deg	
O—Pb—O	89.5(2)	89.3(3)
O→Pb←O	151.7(2)	150.3(2)
O—Pb←O (<i>endo</i>)	70.3(2)	69.1(3), 71.3(3)
O—Pb←O (<i>exo</i>)	89.4(1)	88.6(3), 88.5(3)
Pb—O—C	120.4(4)	122.6(6), 127.0(6)
Pb←O—C	118.4(4)	124.1(7), 112.9(6)
Pb—O→Pb	109.7(2)	110.9(3), 108.7(3)
O—Pb...X	83.9(2), 128.9(2)	81.4(6), 132.4(6) 85.2(6), 129.8(6)
O→Pb...X	59.0(2), 134.0(2)	63.5(6), 131.4(6), 59.4(6), 133.0(6)
X...Pb...X	137.0(2)	135.3(7)

Therefore, it is of interest to consider the problem of $\text{Pb}\dots\text{N}$ coordination in the structure of **3** from the standpoint of vibrational spectroscopy. The optimized geometric parameters of the central fragment of the model compound **3p** appeared to be close to the experimental values determined for structure **3** (see Table 3). In particular, the calculated intermolecular distances $\text{Pb}\dots\text{N}$ in **3p** (3.06 and 3.22 Å) are close to the corresponding experimental values for **3** (3.02 and 3.20 Å). Such distances are usually treated as nonbonding because they are much longer than the similar $\text{N}(\text{sp}^3)\rightarrow\text{Pb}$ coordination bonds in the complexes with six- or seven-coordinate lead atom ($\sim 2.5\text{--}2.6$ Å).²⁴ At the same time, the $\nu_{\text{C-N}}^s$ stretching frequency in the Raman spectrum of compound **3** (780 cm^{-1}) is almost equal to the corresponding frequencies in the spectra of compounds **1**, **2** and **4** whose structures exhibit a distinct intramolecular coordination $\text{N}\rightarrow\text{El}^{\text{II}}$. The sensitivity of the vibrational frequency $\nu_{\text{C-N}}^s$ to the coordination of the N atom was demonstrated both experimentally and theoretically using NCA calculations (see above) not only for $\text{El} = \text{Ge}$ and Sn , but also for $\text{El} = \text{Pb}$. Note that the calculated frequencies $\nu_{\text{C-N}}^s$ of a virtual chelated monomer **3m** with its short distance $\text{N}\rightarrow\text{Pb}^{\text{II}}$ (2.65 Å) and of the polymeric model **3p** with much longer distances $\text{N}\dots\text{Pb}^{\text{II}}$ (3.02 and 3.20 Å) are nearly equal (about 765 cm^{-1}). This means that within the limits studied the frequency of this mode depends only slightly on the $\text{N}\dots\text{Pb}$ distance. Thus, from the standpoint of vibrational spectroscopy, the $\text{N}\rightarrow\text{Pb}$ coordination in structure **3** does occur; this is indirectly proved by the directionality of the LPs of N atoms toward Pb^{II} atoms. When considering the interatomic distances

Pb...N in the structure of **3**, it is pertinent to mention a wide range of the lengths of the secondary bonds Hg...N and Au...N.²⁵ According to Ref. 25, this type of secondary bonds is characterized by directionality and the ability to exhibit a wide range of distances depending on the particular case.

Thus, in the present work, the vibrational spectra of compounds of divalent atoms of Group 14 elements El^{II} = Ge, Sn, Pb, containing the β -dimethylaminoethoxy ligand as the chelating agent, were obtained for the first time and analyzed using NCA calculations. The monomeric compounds El(OCH₂CH₂NMe₂)₂ with El = Ge and Sn were confirmed to be isostructural. Contrary to this, the lead-containing congener is a polymer, as confirmed by X-ray diffraction analysis, and preserves the polymeric structure even in the pyridine solution. The ν^s_{C-N} vibrational frequency in the CH₂NMe₂ group was shown to decrease by 80–100 cm⁻¹ owing to the formation of the coordination bond El←N. At first, the dynamic *flip-flop* process in solutions was modeled as an equilibrium between the stable form with one coordination bond N→El cleaved and the starting molecule.¹ However, the Raman experiments aimed at detecting this process for compounds El^{II}(OCH₂CH₂NMe₂)₂ (El = Ge, Sn) in solutions in THF and Py revealed no "open" form in agreement with the results of energy calculations. A new, more probable mechanism of the dynamic process was proposed, which explains signal broadening in the NMR spectra, *viz.*, an overturn of the CH₂NMe₂ fragment involving cleavage of the El←N bond only in the transition state; studies in this field are now in progress.

This work was financially supported by the Russian Foundation for Basic Research (Project No. 10-03-01115) and the Russian Academy of Sciences (Program of the Division of Chemistry and Materials Science "Theoretical and Experimental Research on the Nature of Chemical Bond and on the Mechanisms of the Key Chemical Reactions and Processes").

References

1. N. N. Zemlyansky, I. V. Borisova, M. G. Kuznetsova, V. N. Khrustalev, Yu. A. Ustynyuk, M. S. Nechaev, V. V. Lunin, J. Barrau, G. Rima, *Organometallics*, 2003, **22**, 1675.
2. *Cambridge Structural Database System*, Release 2009.
3. (a) Y. Mizuhata, T. Sasamori, N. Tokitoh, *Chem. Rev.*, 2009, **109**, 3479; (b) J. Barrau, G. Rima, T. El Amraoui, *Organometallics*, 1998, **17**, 607.
4. N. N. Zemlyansky, I. V. Borisova, V. N. Khrustalev, M. Yu. Antipin, Yu. A. Ustynyuk, M. S. Nechaev, V. V. Lunin, *Organometallics*, 2003, **22**, 5441.
5. V. N. Khrustalev, N. N. Zemlyanskii, I. V. Borisova, M. G. Kuznetsova, E. B. Krut'ko, M. Yu. Antipin, *Izv. Akad. Nauk, Ser. Khim.*, 2007, 259 [*Russ. Chem. Bull., Int. Ed.*, 2007, **56**, 267].
6. N. N. Zemlyanskii, I. V. Borisova, M. S. Nechaev, V. N. Khrustalev, V. V. Lunin, M. Yu. Antipin, Yu. A. Ustynyuk, *Izv. Akad. Nauk, Ser. Khim.*, 2004, 939 [*Russ. Chem. Bull., Int. Ed.*, 2004, **53**, 980].
7. V. N. Khrustalev, I. A. Portnyagin, N. N. Zemlyansky, I. V. Borisova, M. S. Nechaev, Y. A. Ustynyuk, M. Yu. Antipin, V. V. Lunin, *J. Organomet. Chem.*, 2005, **690**, 1172.
8. (a) V. N. Khrustalev, I. A. Portnyagin, N. N. Zemlyansky, I. V. Borisova, Y. A. Ustynyuk, M. Yu. Antipin, *J. Organomet. Chem.*, 2005, **690**, 1056; (b) I. A. Portnyagin, M. S. Nechaev, *J. Organomet. Chem.*, 2009, **694**, 3149; (c) I. A. Portnyagin, Cand. Sci. (Chem.) Thesis, M. V. Lomonosov Moscow State University, 2007 (in Russian); (d) V. N. Khrustalev, I. A. Portnyagin, M. S. Nechaev, S. S. Bukalov, L. A. Leites, *Dalton Trans.*, 2007, 3489.
9. (a) P. Jutzi, S. Keitemeyer, B. Neumann, A. Stammeler, H.-G. Stammeler, *Organometallics*, 2001, **20**, 42; (b) J. Bender IV, M. M. Banaszak, M. M. B. Holl, J. W. Kampf, *Organometallics*, 1997, **15**, 2743; (c) U. Baumeister, H. Hartung, K. Jurkschat, A. Tzschach, *J. Organomet. Chem.*, 1986, **304**, 107; (d) M. Weidenbruch, U. Grobecker, W. Saak, E.-M. Peters, K. Peters, *Organometallics*, 1998, **17**, 5206; (e) H. H. Karsch, *Izv. Akad. Nauk, Ser. Khim.*, 1993, 2025 [*Russ. Chem. Bull. (Engl. Transl.)*, 1993, **42**, 1937]; (f) H. H. Karsch, E. Witt, in *Organosilicon Chemistry III. From Molecules to Materials*, Eds N. Auner, J. Weis, Wiley VCH, Weinheim, Germany, 1998.
10. M. J. S. Gynane, D. H. Harris, M. F. Lappert, P. P. Power, P. Rivière, M. J. Rivière-Baudet, *Dalton Trans.*, 1977, 2004.
11. M. J. Frisch, G. W. Trucks, H. B. Schlegel, G. E. Scuseria, M. A. Robb, J. R. Cheeseman, J. A. Montgomery, Jr., T. Vreven, K. N. Kudin, J. C. Burant, J. M. Millam, S. S. Iyengar, J. Tomasi, V. Barone, B. Mennucci, M. Cossi, G. Scalmani, N. Rega, G. A. Petersson, H. Nakatsuji, M. Hada, M. Ehara, K. Toyota, R. Fukuda, J. Hasegawa, M. Ishida, T. Nakajima, Y. Honda, O. Kitao, H. Nakai, M. Klene, X. Li, J. E. Knox, H. P. Hratchian, J. B. Cross, V. Bakken, C. Adamo, J. Jaramillo, R. Gomperts, R. E. Stratmann, O. Yazyev, A. J. Austin, R. Cammi, C. Pomelli, J. W. Ochterski, P. Y. Ayala, K. Morokuma, G. A. Voth, P. Salvador, J. J. Dannenberg, V. G. Zakrzewski, S. Dapprich, A. D. Daniels, M. C. Strain, O. Farkas, D. K. Malick, A. D. Rabuck, K. Raghavachari, J. B. Foresman, J. V. Ortiz, Q. Cui, A. G. Baboul, S. Clifford, J. Cioslowski, B. B. Stefanov, G. Liu, A. Liashenko, P. Piskorz, I. Komaromi, R. L. Martin, D. J. Fox, T. Keith, M. A. Al-Laham, C. Y. Peng, A. Nanayakkara, M. Challacombe, P. M. W. Gill, B. Johnson, W. Chen, M. W. Wong, C. Gonzalez, J. A. Pople, *GAUSSIAN 03, Revision C.01*, Gaussian, Inc., Wallingford (CT), 2004.
12. J. P. Perdew, K. Burke, M. Ernzerhof, *Phys. Rev. Lett.*, 1996, **77**, 3865.
13. (a) R. Krishnan, J. S. Binkley, R. Seeger, J. A. Pople, *J. Chem. Phys.*, 1980, **72**, 650; (b) L. A. Curtiss, M. P. McGrath, J.-P. Blandeau, N. E. Davis, R. C. Binning, Jr., L. Radom, *J. Chem. Phys.*, 1995, **103**, 6104.
14. (a) K. A. Peterson, *J. Chem. Phys.*, 2003, **119**, 11099; (b) K. A. Peterson, P. Figgen, E. Goll, H. Stoll, M. Dolg, *J. Chem. Phys.*, 2003, **119**, 11113.
15. V. A. Sipachev, *J. Mol. Struct. (THEOCHEM)*, 1985, **121**, 143.

16. *APEX2 Software Package*, v. 1.27, Bruker AXS, Madison, Wisconsin, USA, 2005.
17. G. M. Sheldrick, *Acta Crystallogr.*, 2008, **A64**, 112.
18. (a) G. A. Guirgis, A. M. El Defrawy, T. K. Gounev, M. S. Soliman, J. R. Durig, *J. Mol. Struct.*, 2007, **834**–**836**, 17.
19. (a) L. A. Leites, A. V. Zabula, S. S. Bukalov, A. A. Korlyukov, P. S. Koroteev, O. S. Maslennikova, M. P. Egorov, O. M. Nefedov, *J. Mol. Struct.*, 2005, **750**, 116; (b) L. A. Leites, A. V. Zabula, S. S. Bukalov, P. S. Koroteev, O. S. Maslennikova, M. P. Egorov, O. M. Nefedov, *Izv. Akad. Nauk, Ser. Khim.*, 2005, 1089 [*Russ. Chem. Bull., Int. Ed.*, 2005, **54**, 1117].
20. K. Izod, W. McFarlane, B. Allen, W. Clegg, R. W. Harrington, *Organometallics*, 2005, **24**, 2157.
21. (a) D. O. Harris, G. G. Engerholm, C. A. Tolman, A. C. Luntz, R. A. Keller, H. Kim, W. D. Gwinn, *J. Chem. Phys.*, 1969, **50**, 2438; (b) K. S. Pitzer, W. E. Donath, *J. Am. Chem. Soc.*, 1959, **81**, 3213.
22. A. Haaland, *Angew. Chem., Int. Ed. Engl.*, 1989, **28**, 992.
23. B. Krebs, A. Brommelhaus, B. Kersting, M. Nienhaus, *Eur. J. Solid State Inorg. Chem.*, 1992, **29**, 167.
24. (a) A. B. Ilyukhin, V. B. Logvinova, R. L. Davidovich, *Zh. Neorg. Khim.*, 1999, **44**, 1654 [*Russ. J. Inorg. Chem. (Engl. Transl.)*, 1999, **44**]; (b) E. S. Claudio, M. A. der Horst, C. E. Forde, C. L. Stern, M. K. Zart, H. A. Godwin, *Inorg. Chem.*, 2000, **39**, 1391; (c) J.-G. Mao, Z. Wang, A. Clearfield, *Dalton Trans.*, 2002, 4541; (d) T. I. Ivanova, I. V. Rozhdestvenskaya, V. S. Fundamenskii, I. A. Kasatkin, *Zh. Neorg. Khim.*, 2002, **43**, 125 [*Russ. J. Inorg. Chem. (Engl. Transl.)*, 2002, **43**]; (e) J. Sanchiz, P. Esparza, D. Villagra, S. Dominguez, A. Mederos, F. Brito, L. Araujo, A. Sanchez, J. M. Arrieta, *Inorg. Chem.*, 2002, **41**, 6048; (f) J. Wang, Z.-R. Liu, X.-D. Zhang, W.-G. Jia, D.-M. Fan, *Chinese J. Struct. Chem.*, 2003, **22**, 454; (g) R. L. Davidovich, A. V. Gerasimenko, V. B. Logvinova, *Zh. Neorg. Khim.*, 2004, **49**, 761 [*Russ. J. Inorg. Chem. (Engl. Transl.)*, 2004, **49**]; (h) R. L. Davidovich, A. V. Gerasimenko, V. B. Logvinova, *Zh. Neorg. Khim.*, 2005, **50**, 978 [*Russ. J. Inorg. Chem. (Engl. Transl.)*, 2005, **50**].
25. L. G. Kuz'mina, *Koord. Khim.*, 1999, **25**, 649 [*Russ. J. Coord. Chem. (Engl. Transl.)*, 1999, **25**].

Received May 17, 2010;
in revised form November 12, 2010